ORIGINAL RESEARCH

Vet Record

Performance evaluation of electrode design and material for a large animal electrical impedance tomography belt

Olivia Brabant[1] | **Sarah Loroesch**[1] | **Andy Adler**[2] | **Andreas D. Waldmann**[3] | **Anthea Raisis**[1] | **Martina Mosing**[1]

[1]School of Veterinary and Life Sciences, Murdoch University, Murdoch, Western Australia, Australia

[2]Department of Systems and Computer Engineering, Carleton University, Ottawa, Ontario, Canada

[3]Department of Anaesthesiology and Intensive Care Medicine, Rostock University Medical Centre, Rostock, Germany

Correspondence
Olivia Brabant, School of Veterinary and Life Sciences, Murdoch University, 90 South Street, Murdoch, WA 6150, Australia.
Email: oliviabrabant22@gmail.com

Abstract

Background: Electrical impedance tomography (EIT) produces lung ventilation images via a thoracic electrode belt. Robust electrode design and material, providing low electrode skin contact impedance (SCI), is needed in veterinary medicine. The aim of this study was to compare three EIT electrode designs and materials.

Methods: Simulations of cylindrical, rectangular and spiked electrode designs were used to evaluate electrode SCI as a function of electrode size, where skin contact was uneven. Gold-plated washers (E_{GW}), zinc-plated rivets (E_{ZR}) and zinc-galvanised spikes (E_{ZS}) were assigned randomly on two interconnected EIT belts. Gel was applied to the cranial or caudal belt and placed on 17 standing cattle. SCI was recorded at baseline and 3, 5, 7, 9 and 11 minutes later.

Results: Simulations that involved electrodes with a greater skin contact area had lower and more uniform SCI. In cattle, SCI decreased with all electrodes over time ($p < 0.01$). Without gel, no difference was found between E_{GW} and E_{ZS}, while SCI was higher for E_{ZR} ($p < 0.03$). With gel, SCI was lower in E_{GW} and E_{ZR} ($p < 0.026$), with the SCI in E_{GW} being the lowest ($p < 0.01$).

Limitations: Low numbers of animals and static electrode position may affect SCI.

Conclusions: Electrode design is important for EIT measurement, with larger electrode designs able to compensate for the use of less conductive materials. Gel is not necessary to achieve acceptable SCI in large animals.

KEYWORDS
cattle, electrical impedance tomography, electrode design, electrode size, skin contact impedance

INTRODUCTION

Electrical impedance tomography (EIT) provides a new, non-invasive, radiation-free thoracic imaging modality in animals. An imperceivable alternating electrical current is used to generate dynamic lung images via measurement of impedance change by placing an electrode belt around the thorax.[1–4]

Clinically, EIT can be used as a continuous functional cardiopulmonary monitoring tool to assess ventilation distribution and heart rate in conscious and anaesthetised large animal patients.[5–9] More recently, EIT has been used to evaluate equine asthma and lung changes in horses with left-sided volume overload, and there is potential for expansion of thoracic EIT to illustrate lung pathology in cattle.[10,11]

Skin contact impedance (SCI) is the resistance to this current derived from a complex relationship between the electrode and skin surface and is affected by variations in ion potentials, levels of perspiration and presence or absence of gel.[12–14]

Current for EIT image reconstruction is injected into the skin, and this is achieved in a 'skip' of four patterns. To measure the SCI, voltages from both the driven pairs of electrodes are needed to estimate the SCI. For example, if we wish to gain the SCI for any

given electrode, such as electrode 15, this is stimulated in electrode pairs 10↔15 and 15↔20, and we can measure voltages from both pairings to make an estimation of SCI. By using this method for all electrodes, we can estimate the SCI of each individual electrode.

While there are no specific body boundaries in reconstruction of EIT images, to maximise the sensitivity of the measurement, it has been suggested that minimal SCI should be achieved.[15] In vivo, this is unachievable due to movement changing the conformational boundaries by altering the direction of the vector of current relative to the imaged area, resulting in anomalies.[15] Using a current frequency of 50 kHz, it has been possible to reconstruct images with an SCI of 2000 Ω[12,16,17]; however, the preferred SCI in humans is 100–200 Ω, and an upper limit of 700 Ω has been defined in neonates.[12,16,18] The SCI has not been defined in animals and is likely much higher due to differing properties of the haired skin.[12] It is considered preferable to reduce SCI to minimise the artefact and distortion of images.[15,19]

Electrode size is an important parameter to ensure low SCI. Narrower electrodes have been shown to improve image resolution for changes that are occurring near the body surface close to the electrode,[20] but at depth, such as in the lung, this result cannot be applied. Several mathematical papers have studied electrode models, but do not look at skin contact quality in vivo in detail.[19,21–23]

If the electrode has to fit on a curved uneven surface such as a thorax, a larger electrode area will have a better chance of having some regions with good contact. Furthermore, for a given electrode displacement, a larger electrode area will have less relative movement, which means a larger area is still in contact with the skin. However, a smaller electrode area may be more likely to sit flush and not angled on an uneven skin surface. A spiked design is able to penetrate through the hair and provide a good level of contact under the point of the spike. With multiple spikes on a base making up a single electrode, this might increase surface area, which may provide better overall skin contact. Understanding the size and surface area suitable for an electrode is central for design. This is important when designing electrodes for use in animals with a curved, uneven and haired skin surface.

Electrode design in humans varies between single-use gel electrodes (Goe-MF II, Vyaire, Höchberg, Germany), single-use textile electrode belts (Sentec, Landquart, Switzerland) and reusable small rubber electrodes (PulmoVista 500 Dräger, Lübeck, Germany).[18,24,25] These designs of small, individual, single-use gel and fabric electrodes are unsuitable for densely haired animals or for use in field settings.

Material is another principal component when constructing a cost-efficient reusable EIT electrode for use in large animals. Gold has proved to be useful in medical and electronic equipment and should exhibit the lowest resistivity to current.[26,27] It is highly conductive, chemically stable, non-corrosive and used as an electrode material to perform EIT measurements in large animals.[25,28] Furthemore, gold has been shown to reduce SCI compared with stainless-steel composites.[28,29] However, gold is approximately six and 13 times more expensive than zinc-plated rivets and zinc-galvanised spikes, respectively. Alternative electrode material may improve cost efficiency while still providing adequate SCI for image reconstruction.

Water alone, applied to the skin's surface to reduce SCI, has been used for EIT in the field in large animals; however, the application of low-conductive ultrasound gel has been shown to further reduce electrode SCI for ECG measurements in cattle.[30,31] The addition of gel for EIT measurements might be especially important in haired animals, but it increases the cost of the procedure.

The points raised above highlight the necessity of finding a robust, reusable and cost-effective electrode material with a design that is capable of providing adequately low SCI through haired skin in large animals.

This study aimed to compare electrode size and design in a mathematical simulation followed by an experimental animal study based on the simulation results using cattle as a large animal model. Furthermore, we aimed to measure the effect of gel application on SCI.

MATERIALS AND METHODS

Part A: Simulations

Before the experimental animal study, the electrode size was addressed via simulations of three electrode types: cylindrical, rectangular and spiked. Simulations were performed in Electrical Impedance Tomography and Diffuse Optical Tomography Reconstruction Software (EIDORS)[32] and Netgen.[33] Finite element models of an electrode–skin interface were created for theoretical electrode designs (Figure 1). The skin-surface properties were varied to represent the non-homogeneous properties of the skin, with fatty (non-conductive) regions traversed by more
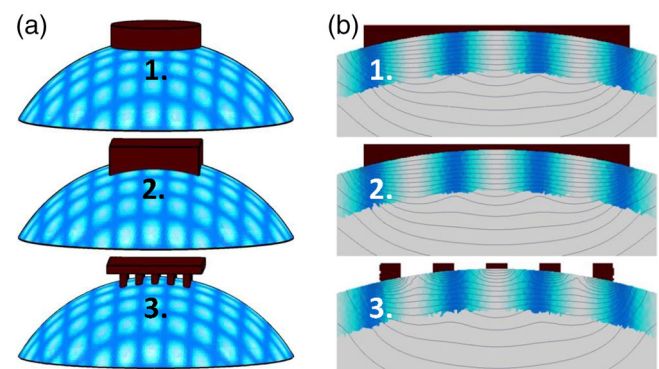

FIGURE 1 Finite element models of electrode configurations. (a) (1) Cylindrical, (2) rectangular and (3) spiked conductive electrodes (red) connected to a semi-spherical body model. The body's outer layer is patterned into a mix of non-conductive (blue) and more conductive (white) regions simulating differing skin contact quality. (b) Equipotential lines showing voltage distribution underneath (1) cylindrical, (2) rectangular and (3) spiked electrodes. Note the variations in equipotential due to the non-conductive skin regions (blue)
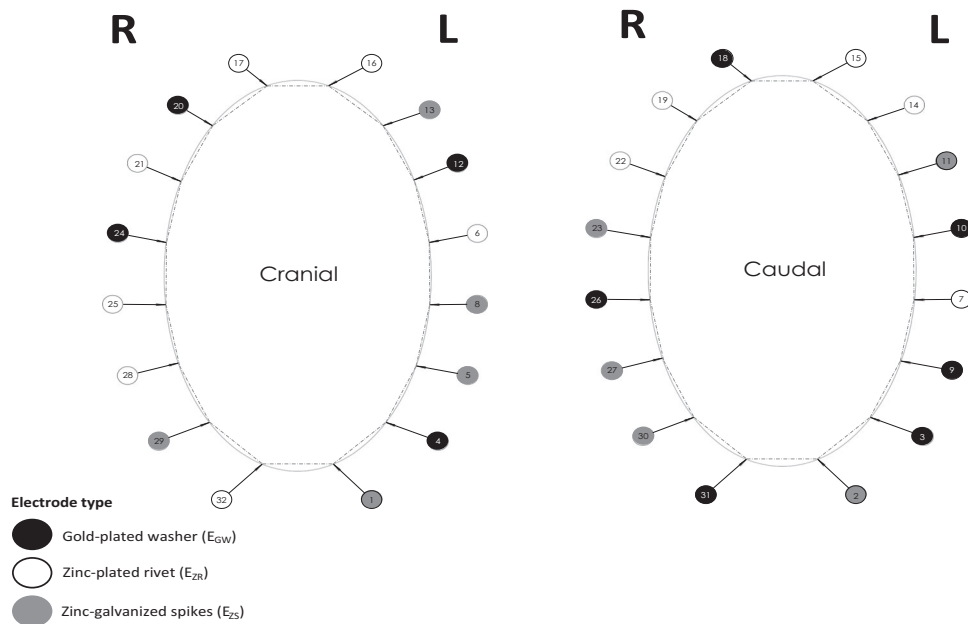
FIGURE 2 Schematic of the cranial and caudal belt layouts illustrating electrode number and position. Left and right have been identified to correspond to positioning on the animal. The electrode number and type have been shown as gold-plated washer (E_{GW}) (black), zinc-galvanised steel spike (E_{ZS}) (white) and zinc-plated rivet (E_{ZR}) (grey)

conductive areas such as sweat and other pores. No anatomical model of the variability was available, but instead a representative grid of spatial variation in skin properties on a curved surface was created to represent the thorax (Figure 1). The current propagation underneath the three types of electrodes was shown via equipotential lines to illustrate areas of skin contact (Figure 1). Four different surface areas (0.10, 0.15, 0.20 and 0.25 cm^2) were created for the three different electrode types, and the SCI was assessed at each surface area.

Part B: Experimental animal study

Electrodes

Three electrode designs (a round flat washer [$d_{28\,mm} \times D_{3\,mm}$], a rectangular spiked panel [$H_{37\,mm} \times W_{33\,mm} \times D_{10\,mm}$] and a raised round rivet [$d_{16\,mm} \times D_{4\,mm}$]) and three materials (gold plating, galvanised zinc and plated zinc) were selected based on the materials available for testing (Figures 2 and 3). The gold-plated washers were acquired from Gold-Parts (Oldendorf, Germany) and represent the theoretically best design and material based on the mathematical simulations. The zinc electrodes were selected from commercially available, inexpensive, robust materials (Bunnings, Australia). The gold-plated washers (E_{GW}) ($n = 10$), zinc-galvanised spikes (E_{ZS}) ($n = 10$) and zinc-plated rivets (E_{ZR}) ($n = 12$) were randomly assigned to one of 32 positions on one of two interconnected electrode belts using a random number generator (randomizer.org) (Figure 2). These two electrode belts were subsequently connected to a cable belt containing wiring linked to the EIT hardware, resulting in a cranial (E_{GW} [$n = 4$], E_{ZS} [$n = 5$], E_{ZR} [$n = 7$]) and caudal
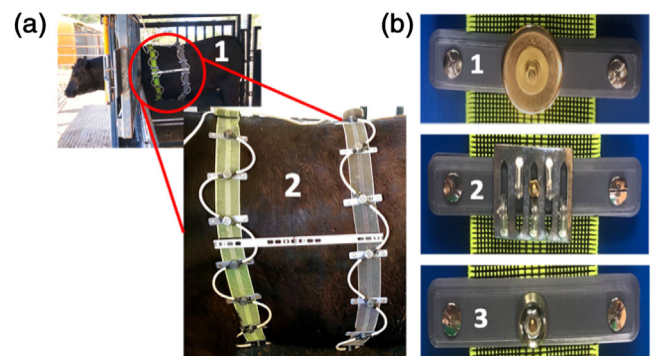

FIGURE 3 Example of the electrical impedance tomography (EIT) belt in use and the individual electrode types used in the study. (a) Two interconnected EIT belts in situ: (1) belt on standing cow within a crush, and (2) close-up of two belts with spacer in place. (b) Individual electrodes mounted to a grey plastic bracket for stability: (1) gold-plated washer (E_{GW}) ($d_{28\,mm} \times D_{3\,mm}$), (2) zinc-galvanised steel spike (E_{ZS}) ($H_{37\,mm} \times W_{33\,mm} \times D_{10\,mm}$) and (3) zinc-plated rivet (E_{ZR}) ($d_{16\,mm} \times D_{4\,mm}$)

(E_{GW} [$n = 6$], E_{ZS} [$n = 5$], E_{ZR} [$n = 5$]) EIT belt with 16 electrodes on each (Figures 2 and 3).

Animals

Seventeen female adult mixed-breed cattle with a mean age of 5.4 years (SD ± 1), weighing 655 kg (SD ± 97.2) and with a mean body condition of 4 (SD ± 0.66) (thin–obese: 1–5), were assigned to participate in the study. A power calculation, using a significance of 0.05 and 95% confidence limits, suggested a minimum of 12 cows. Before the study, the cows were on pasture with the rest of the herd before being brought to the cattle yard. Each cow was restrained in a standing position within a crush. The thorax of each cow was hosed down with water before belt placement.

Instrumentation and data collection

Cow temperament score (1—quiet [standing quietly in the crush] to 4—agitated [kicking and constant movement]) was recorded prior to belt placement. If any cow reached a score of 4 at any point during the study, data collection was terminated, the equipment was removed and the cow was returned to the herd.

The belt was prepared by connecting the electrode belt to the cable belt via the clip fastenings, and low-conductive ultrasound gel (Aquasonic, Fairfield, CT, USA) was applied randomly to either the cranial or caudal belt (randomizer.org). The belt was then placed on the cow.

First, the cranial belt was placed vertically at the level of the fifth to sixth intercostal space, and then the caudal belt 40 cm caudally at the level of the ninth to tenth intercostal space. Both the belts were passed over the cow and then fastened at the dorsal aspect. The belt was then connected to an EIT device (Sentec), which was connected to a laptop for data recording.

Individual electrode SCI and electrode failure were measured directly after the belt was placed and connected to the EIT device, at baseline (TBL) and 3, 5, 7, 9 and 11 minutes later (T3–T11). Electrode failure was identified where there was a visibly detached electrode or where a loss of signal was detected (indicated by a red icon on the individual electrode in the STEM software [Sentec]).

During each timepoint, electrode SCI measurements (in Ω) of each electrode were recorded using STEM software.

After the final measurement, the belts were removed, the skin was examined for damage and any damage was recorded. Skin damage was measured using a four-point scale, where 0 indicated no marks where the belt was placed, no skin redness and cow compliant with touch, and 3 indicated marks easily visible where the belt was placed, some damage to the skin and moderate to severe reaction to touch. The cow was then released from the crush and returned to the herd.

Data analysis

The SCI measurements from the STEM software were entered retrospectively, along with the electrode failures, into an excel spreadsheet (Microsoft, USA) for further analysis.

Statistical analysis

Statistical analysis was performed using SPSS (IBM SPSS Statistics, Version 27, NY, USA). Results are given as mean ± standard deviation (SD). Statistical significance was set at $p < 0.05$. Descriptive interpretation has been provided from the EIDORS output for the simulations.

All statistics were calculated from the means of the three electrode types on each belt in each cow over time except for the simulations. Data from the animal study were assessed for normality using a Kolmogorov–Smirnov test. One-way ANOVA of repeated measures was performed on the averaged SCI measurements, and Tukey's honestly significant difference test was used for multivariant analysis between electrode types at each timepoint. No gel versus gel was assessed with a paired T-test at each timepoint. Measurements of failing electrodes were excluded and evaluated separately for reasons of failure.

RESULTS

Simulations

Simulations calculated electrode-to-body SCI through the electrode as a function of electrode size (Figure 1). These simulations revealed that larger electrodes had lower and more uniform SCI for each area (Figure 4). An area of 0.10 cm^2 had a high SCI for all electrode designs, this increased as the contact surface, represented by the ($\sigma_{max}/\sigma_{min}$) ratio, became more uneven (Figure 4). An area of 0.25 cm^2 exhibited the lowest SCI for all electrode designs, with less influence on SCI as the contact surface became more uneven. The spiked design had the highest SCI at all areas and was exacerbated where the area was small (ie, 0.1 and 0.15 cm^2) (Figure 4).

Experimental animal study

Mean temperament score was 1.25 ± 0.43 and was consistent across all cows. No damage to the skin was noted after removal of the belt in any location or cow.

A total of 3264 from 3357 electrode SCI recordings were included in the statistical analysis. The remaining 93 recordings were electrode failures, which were removed from the statistical analysis and analysed separately.

Results are given as mean and SD for overall SCI measurements: E_{GW} 285.92 ± 48.07 Ω, E_{ZS} 319.48 ± 83.80 Ω and E_{ZR} 392.21 ± 27.40 Ω (Table 1). Electrode SCI in all three electrodes decreased over time with and without gel ($p < 0.01$).

Without gel, no significant difference in electrode SCI was seen overall (Table 1). The SCI in E_{ZR} was significantly higher at T3, T4, T5 and T6 and T2, T3, T4, T5 and T6 compared to E_{GW} and E_{ZS}, respectively (Figure 5).

With the addition of gel, SCI was significantly lower in the E_{GW} ($p < 0.017$) and E_{ZR} ($p < 0.026$) electrode designs at all timepoints compared with no gel. This difference was not seen with the E_{ZS} electrode design. The SCI was significantly lower in E_{GW} at T4, T5 and T6 when compared to E_{ZR} (Figure 5). No differences were observed between E_{GW} and E_{ZS} or between E_{ZR} and E_{ZS} (Table 1).

Failing electrodes were registered ($n = 93$). These electrodes were all located at the level of the lower third of the thorax on the caudal aspect of the belt (cranial belt electrodes 8, 24, 29; caudal belt electrodes 3,
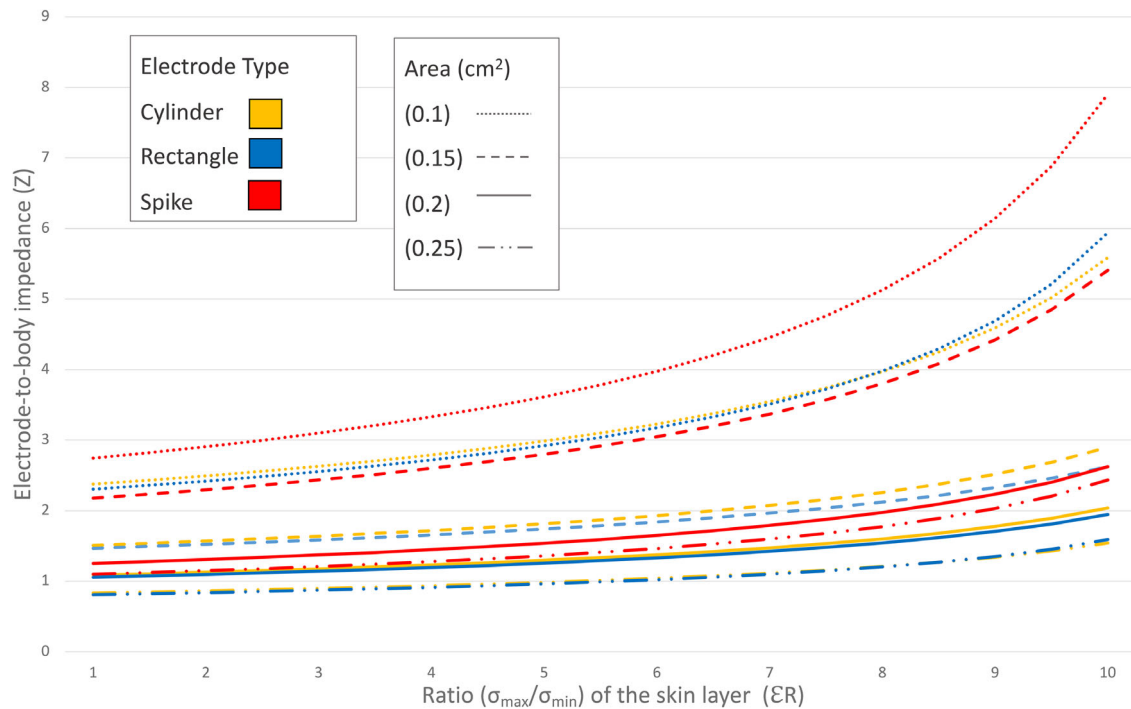
FIGURE 4 Electrode-body impedance of the three electrode shapes defined in Figure 2. X-axis is the ratio ($\sigma_{max}/\sigma_{min}$) of the skin layer and describes the variability of conductivity of the skin. Four different electrode areas (0.10, 0.15, 0.2 and 0.25 cm^2) are shown for each electrode type, corresponding to the various lines showing variability in electrode-to-body contact impedance as area increases

TABLE 1 Mean and standard deviation (SD) of skin contact impedance, measured in ohm (Ω), for three electrode types: gold-plated washer (E_{GW}), zinc-galvanised steel spike (E_{ZS}) and zinc-plated rivet (E_{ZR})

Electrode type	Skin contact impedence (mean $\pm$ SD) (Ω)		
	Overall	Without gel	With gel
Gold-plated washer (E_{GW})	285.92 $\pm$ 48.07	335.44 $\pm$ 130.17	231.06 $\pm$ 120.02
Zinc-galvanised steel spike (E_{ZS})	319.48 $\pm$ 83.80	325.96 $\pm$ 89.46	310 $\pm$ 143.32
Zinc-plated rivet (E_{ZR})	392.21 $\pm$ 27.40	453.03 $\pm$ 138.57	334.17 $\pm$ 109.25

7, 10) (Figure 2). Failure was directly associated with mechanical impact on the electrodes in these locations (crush bars detaching the EIT cable from the actual electrode) and was therefore not statistically analysed for design.

DISCUSSION

Our study shows that electrode size, design and material are important for EIT measurements in large animals. Electrodes with a larger surface area of 0.2–0.25 cm^2 are more suitable for an uneven skin surface. A round washer or rectangular spiked design, using gold plating or zinc-galvanised materials, achieves the SCI needed for EIT measurements.

In our study, simulations revealed that electrodes with a larger surface area have lower and more uniform SCI (Figures 1 and 3). The spiked design in the simulation had the largest surface area; however, the points of body contact were fewer. This caused an increased bending of electrical potentials and voltage distribution around non-conductive body regions (Figure 1). This resulted in a marginally higher SCI

than either the cylindrical or the rectangular design at all surface areas, yet was comparable to a flat electrode at larger surface areas, with the added benefit of being able to penetrate haired skin (Figure 3). Therefore, if a spiked design is to be used, an electrode base area or increased number of spikes will be required to provide suitable SCI. Our subsequent designs from these simulations had the surface area of the spiked design larger than the surface area of the round washer and raised round rivet. The resulting experimental data showed that spikes overcame the surface area issue, maybe by having contact not only with the tip of spike but also other parts of the spikes or even the electrode base area penetrating through hair.

We decided on a smaller round rivet and a larger gold-plated washer to evaluate if a small area may combat the uneven surface of the thorax when sitting flush on the skin. We had to reject our assumption that the tight-sitting design of a smaller electrode may compensate for its reduced surface area, as smaller round rivet electrodes had higher SCI and therefore were less suitable for large animal EIT. This was confirmed in our simulation, as when the electrode area was less than 0.2 cm^2 the resulting SCI was higher.
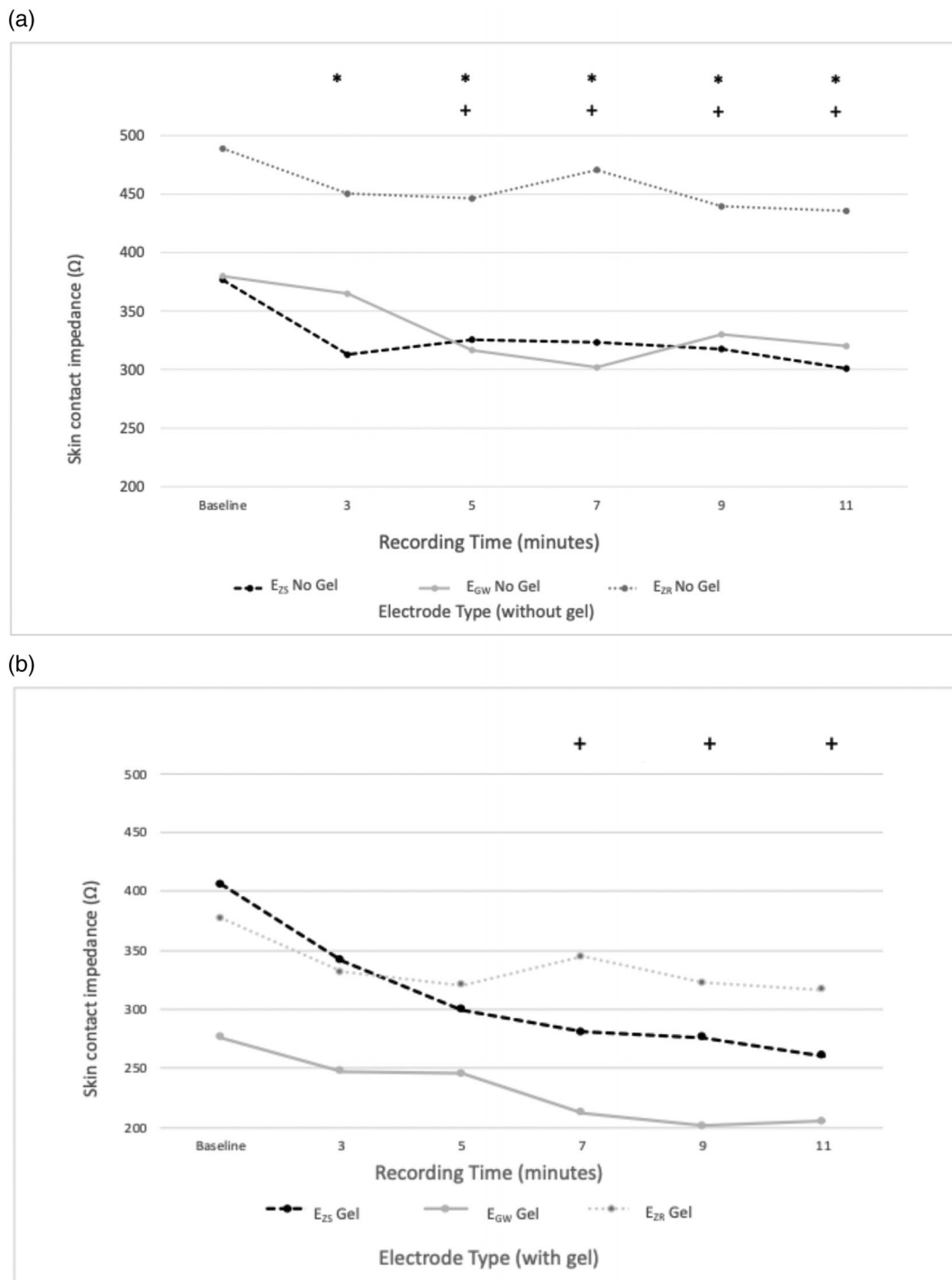
(a)

(b)

FIGURE 5 Line graphs of skin contact impedance (SCI) at all timepoints ($n = 17$ cows in standing position). Graph (a) represents the mean SCI over time for three electrodes: gold-plated washer (E_{GW}), zinc-galvanised steel spike (E_{ZS}) and zinc-plated rivet (E_{ZR}) without gel. $^+p < 0.05$ for differences between E_{GW} and E_{ZR}; $^*p < 0.05$ differences between E_{ZR} and E_{ZS}. Graph (b) represents the mean SCI over time for E_{ZS}, E_{GW} and E_{ZR} with gel. $^+p < 0.05$ for differences between E_{GW} and E_{ZR}

Robust electrode design is crucial for further research in veterinary EIT.[3] Limited work exploring electrode design in the context of human medicine exists, but no such work has previously been performed in a veterinary context.[18] In this study, the design of the electrodes was based on our mathematical simulations and on previous EIT electrode designs reported for use in animals. Earlier work has used washers or other flat electrodes in dogs,[34] pigs,[35] horses[5] and cows.[36] In our study, the spiked design showed SCI similar to the flat washer; therefore, it could be a suitable future design for EIT in animals.

Gold proved to have the lowest SCI; however, gold is the most expensive material. In veterinary medicine, a cheaper alternative would be more desirable. We decided to choose zinc for our study due to its availability, cost efficiency, durability to corrosion and ability to conduct electricity.[27,37–39] Zinc galvanising and zinc plating are two methods of covering steel with zinc, with plating resulting in a thinner zinc coating than galvanising.[40] In our study, gold plating

provided minimal SCI due to its electrical conductivity,[39] but zinc-galvanised steel had a comparable SCI with a spike design, meaning that electrode design can compensate for the lower conductivity of the material.

Using two interconnected electrode belts with an equal number of electrodes allowed the comparison of gel and no gel for the same breath in each cow. To compensate for the difference in anatomical features between the cranial and caudal belts, the usage of gel was randomised to either belt on each cow. Our results agree with the literature for other medical uses of gel, which show that contact quality is improved with the addition of gel.[30,31,41] The reduction in SCI was significant in both E_{GW} and E_{ZR}, with the gel reducing the signal loss from skin to the electrode via a reduction in the air pocket between electrode and skin. This was not seen in the spiked design as the gel may have been unable to reduce the air pockets between the spikes and the skin as the point of contact for each spike is small, therefore not improving the skin-to-electrode contact. The use of a low-conductivity water-based gel reduces the corrosion of the electrodes, increases the electrical impedance from the electrode to skin and is less likely to cause skin irritation, seen in some human patients.[42,43] However, gel increases the cost of use, measurement time and application risk, which can be higher in large animals. Therefore, we questioned whether gel is necessary in addition to wetting the skin with water. Our results suggest wetting of the skin alone is sufficient for practical image reconstruction for EIT; however, the addition of gel does significantly reduce SCI where there is a flat electrode surface in the E_{GW} and E_{ZR} electrodes. This will lead to an increase in EIT image reconstruction quality, which means that variables of ventilation distribution measured via EIT, such as regional ventilation delay, dependent/non-dependent silent spaces and centre of ventilation, can be reconstructed more accurately.[18,44]

Limitations arose with electrode position on the body of the cow. Electrode position did not change between measurements, belt or subject as the same electrode belts were used throughout the study period. This resulted in the same electrodes consistently disconnecting from the skin due to anatomical features or collision with the crush. This contributed to the disconnection between the electrode and cable resulting in electrode failures. As these are mechanical issues rather than material and design features, failures were removed from the analysis.

Skin damage might be a concern with the use of EIT,[45] especially when 'aggressive' electrode designs such as spikes are used. Additionally, flat washers may be less likely to cause skin damage than a spike when a large animal is recumbent under anaesthesia. In the current study, we did not observe any skin damage with either design, as we assessed only cows in a standing position. The authors speculate that, in recumbency, the weight of the large animal on the spike may lead to some degree of skin damage and would need to be explored in future studies.

In conclusion, improved design and less adequate material or less favourable design and more suitable material are appropriate for EIT measurements in standing large animal. Gel provides reduced skin resistance in all electrodes irrespective of design or material; however, image reconstruction is still possible without gel. Our results will aid in belt design and clinical application for functional EIT usage in animals.

AUTHOR CONTRIBUTIONS

ACKNOWLEDGEMENTS

CONFLICTS OF INTEREST

The authors declare they have no conflicts of interest.

FUNDING INFORMATION

DATA AVAILABILITY STATEMENT

The data that support the findings of this study are available from the corresponding author upon reasonable request.

ETHICS STATEMENT

The research was approved by the Murdoch University Ethics Committee at Murdoch University (ref. R3275/20). The Australian code for the care and use of animals for scientific purposes were followed.

ORCID

Olivia Brabant https://orcid.org/0000-0003-0094-2914

REFERENCES

1. Frerichs I, Amato MBP, van Kaam AH, Tingay DG, Zhao Z, Grychtol B, et al. Chest electrical impedance tomography examination, data analysis, terminology, clinical use and recommendations: consensus statement of the translational EIT development study group. Thorax. 2017;72(1):83.
2. Adler A, Arnold JH, Bayford R, Borsic A, Brown B, Dixon P, et al. GREIT: a unified approach to 2D linear EIT reconstruction of lung images. Physiol Meas. 2009;30(6):S35.
3. Adler A, Holder DS. Electrical impedance tomography. 2nd ed. Boca Raton, FL: CRC Press; 2021. p. 290–300.
4. Frerichs I, Schmitz G, Pulletz S, Schädler D, Zick G, Scholz J, et al. Reproducibility of regional lung ventilation distribution determined by electrical impedance tomography during mechanical ventilation. Physiol Meas. 2007;28(7): S261–7.
5. Mosing M, Waldmann A, Raisis A, Böhm S, Drynan E, Wilson K. Monitoring of tidal ventilation by electrical impedance

tomography in anaesthetised horses. Equine Vet J. 2018;51(2):222–6.

6. Schramel J, Nagel C, Auer U, Palm F, Aurich C, Moens Y. Distribution of ventilation in pregnant Shetland ponies measured by electrical impedance tomography. Respir Physiol Neurobiol. 2012;180(2–3):258–62.

7. Ambrisko T, Schramel J, Adler A, Kutasi O, Makra Z, Moens Y. Assessment of distribution of ventilation by electrical impedance tomography in standing horses. Physiol Meas. 2015;37(2):175.

8. Ambrosio AM, Carvalho-Kamakura TPA, Ida KK, Varela B, Andrade FSRM, Facó LL, et al. Ventilation distribution assessed with electrical impedance tomography and the influence of tidal volume, recruitment and positive end-expiratory pressure in isoflurane-anesthetized dogs. Vet Anaesth Analg. 2017;44(2):254–63.

9. Raisis AL, Mosing M, Hosgood GL, Secombe CJ, Adler A, Waldmann AD. The use of electrical impedance tomography (EIT) to evaluate pulse rate in anaesthetised horses. Vet J. 2021;273:105694.

10. Secombe C, Waldmann AD, Hosgood G, Mosing M. Evaluation of histamine provoked changes in airflow using electrical impedance tomography in horses. Equine Vet J. 2020;52(4):556–63.

11. Sacks M, Byrne DP, Herteman N, Secombe C, Adler A, Hosgood G, et al. Electrical impedance tomography to measure lung ventilation distribution in healthy horses and horses with left-sided cardiac volume overload. J Vet Intern Med. 2021;35(5):2511–23.

12. Nguyen D, Kosobrodov R, Barry M, Chik W, Jin C, Oh T, et al. Electrode-skin contact impedance: in vivo measurements on an ovine model. J Phys Conf Ser. 2013;434:012023.

13. Boverman G, Isaacson D, Newell JC, Saulnier GJ, Kao T-J, Amm BC, et al. Efficient simultaneous reconstruction of time-varying images and electrode contact impedances in electrical impedance tomography. IEEE Trans Biomed Eng. 2017;64(4):795–806.

14. Clemente F, Arpaia P, Manna C. Characterization of human skin impedance after electrical treatment for transdermal drug delivery. Measurement. 2013;46(9):3494–501.

15. Boyle A, Adler A. The impact of electrode area, contact impedance and boundary shape on EIT images. Physiol Meas. 2011;32(7):745–54.

16. Boone K, Holder D. Effect of skin impedance on image quality and variability in electrical impedance tomography: a model study. Med Biol Eng Comput. 1996;34(5):351–4.

17. Brazey B, Haddab Y, Zemiti N. Robust imaging using electrical impedance tomography: review of current tools. Proc Royal Soc A. 2022;478(2258):20210713.

18. Sophocleous L, Frerichs I, Miedema M, Kallio M, Papadouri T, Karaoli C, et al. Clinical performance of a novel textile interface for neonatal chest electrical impedance tomography. Physiol Meas. 2018;39(4):044004.

19. Darbas M, Heleine J, Mendoza R, Velasco AC. Sensitivity analysis of the complete electrode model for electrical impedance tomography. AIMS Math. 2021;6(7):7333–66.

20. Yan W, Hong S, Chaoshi R. Optimum design of electrode structure and parameters in electrical impedance tomography. Physiol Meas. 2006;27(3):291–306.

21. Hua P, Woo EJ, Webster JG, Tompkins WJ. Finite element modeling of electrode–skin contact impedance in electrical impedance tomography. IEEE Trans Biomed Eng. 1993;40(4):335–43.

22. Mueller JL, Isaacson D, Newell JC. A reconstruction algorithm for electrical impedance tomography data collected on rectangular electrode arrays. IEEE Trans Biomed Eng. 1999;46(11):1379–86.

23. Wang H. Optimum design of the structure of the electrode for a medical EIT system. Meas Sci Technol. 2001;12(8):1020–3.

24. Putensen C, Hentze B, Muenster S, Muders T. Electrical impedance tomography for cardio-pulmonary monitoring. J Clin Med. 2019;8(8):1176.

25. Gaggero PO, Adler A, Brunner J, Seitz P. Electrical impedance tomography system based on active electrodes. Physiol Meas. 2012;33(5):831.

26. Lide DR. CRC handbook of chemistry and physics : a ready-reference book of chemical and physical data. 82nd ed. Boca Raton, FL/London: CRC Press; 2001.

27. Lobodzinski SS, Laks M. New material for implantable cardiac leads. J Electrocardiol. 2009;42(6):566–73.

28. Bera TK, Nagaraju J. Gold electrode sensors for electrical impedance tomography (EIT) studies. In: IEEE Sensors Application Symposium 2011 (IEEE SAS 2011), 22–24 February, USA. 2011. p. 24–8.

29. Rahal M, Khor JM, Demosthenous A, Tizzard A, Bayford R. A comparison study of electrodes for neonate electrical impedance tomography. Physiol Meas. 2009;30(6):S73.

30. Dry contact electrodes performance in canine ECG. In: Virtanen J, Leivo J, Vehkaoja A, Somppi S, Törnqvist H, Fiedler P, et al., editors. Proceedings of the Fifth International Conference on Animal–Computer Interaction. 2018.

31. Hallowell GD, Potter TJ, Bowen IM. Methods and normal values for echocardiography in adult dairy cattle. J Vet Cardiol. 2007;9(2):91–8.

32. Adler A, Lionheart WR. Uses and abuses of EIDORS: an extensible software base for EIT. Physiol Meas. 2006;27(5):S25.

33. Schöberl J. NETGEN: an advancing front 2D/3D-mesh generator based on abstract rules. Comput Visual Sci. 1997;1(1):41–52.

34. Adler A, Amyot R, Guardo R, Bates JH, Berthiaume Y. Monitoring changes in lung air and liquid volumes with electrical impedance tomography. J Appl Physiol. 1997;83(5):1762.

35. Grychtol B, Elke G, Meybohm P, Weiler N, Frerichs I, Adler A. Functional validation and comparison framework for EIT lung imaging. PLoS One. 2014;9(8):e103045.

36. Brabant O, Crivellari B, Hosgood G, Raisis A, Waldmann AD, Auer U, et al. Effects of PEEP on the relationship between tidal volume and total impedance change measured via electrical impedance tomography (EIT). J Clin Monit Comput. 2022;36(2):325–34.

37. Asri NF, Husaini T, Sulong AB, Majlan EH, Daud WRW. Coating of stainless steel and titanium bipolar plates for anticorrosion in PEMFC: a review. Int J Hydrogen Energy. 2017;42(14):9135–48.

38. Higashi S, Lee SW, Lee JS, Takechi K, Cui Y. Avoiding short circuits from zinc metal dendrites in anode by backside-plating configuration. Nat Commun. 2016;7(1):1–6.

39. Goodman P. Current and future uses of gold in electronics. Gold Bull. 2002;35(1):21–6.

40. Toseland P. Zinc coatings. Product treatment & finishing. Springer; 1972. p. 97–103.

41. The electrical characteristics of electroconductive gels used in biomedical applications. In: Kara S, Konal M, Ertaş M, Uzunoğlu CP, editors. 2017 Medical Technologies National Congress (TIPTEKNO). IEEE; 2017.

42. Ferasin L, Amodio A, Murray JK. Validation of 2 techniques for electrocardiographic recording in dogs and cats. J Vet Intern Med. 2006;20(4):873–6.

43. Cochran R, Rosen T. Contact dermatitis caused by ECG electrode paste. South Med J. 1980;73(12):1667–8.

44. Waldmann AD, Wodack KH, März A, Ukere A, Trepte CJ, Böhm SH, et al. Performance of novel patient interface for electrical impedance tomography applications. J Med Biol Eng. 2017;37(4):561–6.

45. McAdams E, Jossinet J, Lackermeier A, Risacher F. Factors affecting electrode–gel–skin interface impedance in electrical impedance tomography. Med Biol Eng Comput. 1996;34(6):397–408.